Original Article

Institution of MECHANICAL ENGINEERS
Journal of ENGINEERING TRIBOLOGY

Proc IMechE Part J:
J Engineering Tribology
2021, Vol. 235(4) 748–757

DOI: 10.1177/1350650120925582
journals.sagepub.com/home/pij
SAGE

Artificial neural network modeling of sliding wear

Ivan I Argatov[1] and Young S Chai[2]

Abstract

A widely used type of artificial neural networks, called multilayer perceptron, is applied for data-driven modeling of the wear coefficient in sliding wear under constant testing conditions. The integral and differential forms of wear equation are utilized for designing an artificial neural network-based model for the wear rate. The developed artificial neural network modeling framework can be utilized in studies of wearing-in period and the so-called true wear coefficient. Examples of the use of the developed approach are given based on the experimental data published recently.

Keywords

Wear coefficient, sliding wear, artificial neural network, specific wear rate, aluminum alloy matrix composites

Date received: 29 December 2019; accepted: 30 March 2020

Introduction

In recent years, artificial neural networks (ANNs) have emerged as a powerful mathematical tool for data-driven modeling in mechanical[1,2] and structural[3–6] engineering as well as in tribology[7,8] and machine tool treatment.[9–11] In particular, a number of studies[12,13] have employed neural networks for analysis of wear tests.

However, in applications of ANNs to modeling of sliding wear, there are some issues that are of critical importance for interpreting the constructed ANN models and understanding the obtained experimental results.[14] One of the main obstacles associated with applications of ANNs to physical processes like wear is the difficulty of explaining functional interrelations (between the wear rate and the physical variables governing the process) as they are predicted by ANN approximations.[15,16]

To address this so-called "black box" issue of ANN modeling approach, a number of problem-specific ANN-based models of hybrid type have been developed.[17–19] In the present paper, we consider the main problem associated with the application of multilayer perceptron (MLP) for analyzing experimental data obtained from pin-on-disk sliding wear tests. Notwithstanding that MLPs, which is a standard neural network technique, the novelty of our approach, in particular, lies in the way how the coefficient of wear is determined.

Recall that a straightforward approach for the analysis of sliding wear is based on Archard's equation of wear[20] of the form

$$\dot{w} = kpv \tag{1}$$

where p is the contact pressure, v is the sliding velocity, k is the wear coefficient, w is the linear wear (usually measured in microns), and a dot denotes differentiation with respect to time, so that $\dot{w}$ is the (linear) wear rate.

The pin-on-disk test is regarded as one of the standard wear test methods,[21] though its selection should be justified in order to provide a reasonable simulation of a tested tribosystem.[22] From a mathematical modeling point of view, the major advantage of the test scheme with cylindrical pin is that it facilitates the evaluation of a material's wear resistance under constant contact area, while the discrepancy in distribution of relative sliding velocity across the circular contact is insignificant for relatively small pins compared to the disc radius. Moreover, the condition of constant area of contact implies that, when the effect of wear takes place, the contact pressure tends to become uniform across the entire contact.[23]

[1]Institut für Mechanik, Technische Universität Berlin, Berlin, Germany
[2]School of Mechanical Engineering, Yeungnam University, Gyeongsan, South Korea

Corresponding author:
Young S Chai, School of Mechanical Engineering, Yeungnam University, Gyeongsan 38541, South Korea.
Email: yschai@yu.ac.kr

Therefore, the wear coefficient k, which is determined using equation (1), can be regarded as a tribosystem property that is independent of the contact area.

Observe that the Archard equation (1) states that the coefficient of wear k is a characteristic of the tested material, and may also depend on the operational conditions (e.g. pin temperature, sliding velocity, and pressure). This circumstance can be illustrated by the black-box scheme shown in Figure 1. However, equation (1) tentatively suggests that k may be a function of time as well, though the black-box scheme does not reflect this assumption.

Usually, the value of k is determined from experiments conducted under constant normal load, L, and sliding velocity, v, so that k is taken to be proportional to the ratio of wear volume loss, V, to the corresponding sliding distance, s. In other words, in steady state, equation (1) can be written as $V = kLs$, provided that k is a constant with respect to s. It is to recall here that the ratio $V/(Ls)$ is called the specific wear rate (SWR). Therefore, assuming now that k may depend on sliding distance (or time of sliding), the standard approach yields the average value $V/(Ls)$ for the wear coefficient, and this issue should be taken into account in the ANN design (see Figure 2). The wear coefficient that determines the instantaneous wear rate will be called the true wear coefficient.

On the other hand, having constructed an ANN model that relates the wear volume V to the sliding distance s, both of which are extensive variables, one can then raise the question: how to extract the wear equation that relates the wear rate $\dot{w}$ to the operational conditions, which are described by the intensive variables like p and v, thereby getting rid of the dependence on time or sliding distance?

Thus, having been introduced "true" wear coefficient, which may vary during sliding under the constant operational conditions, and its average value, which is provided by the specific wear rate $\mathrm{SWR} = V/(Ls)$, the problem arises how to distinguish the two quantities in ANN modeling. While the majority of publications[8,24,25] use the SWR for estimating the wear coefficient, the present paper apparently constitutes the first integrated attempt to model the true wear coefficient in the ANN framework. We illustrate the use of the developed approach by several examples, which are based on the experimental data fully published in recent papers.

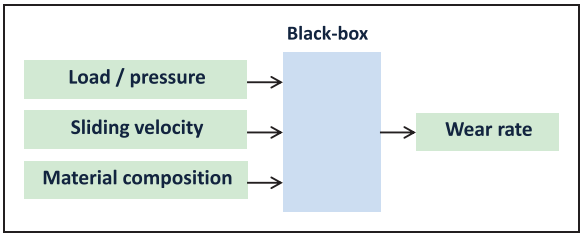

Figure 1. Black-box scheme illustrating the wear equation in differential form.

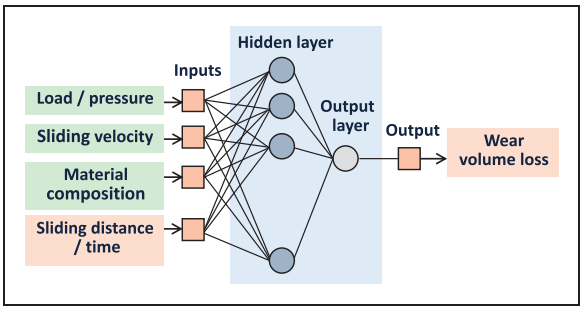

Figure 2. ANN diagram illustrating the wear equation in integral form.

Research significance

The main research implication of this study is that it highlights the modeling aspect of the ANN technique with application to the analysis of sliding wear tests. The mathematical modeling approach is based on the integral and differential forms of Archard's equation of wear, which distinguish between the true wear coefficient (TWC), which is regarded as a function of sliding distance, and the SWR. It is shown that the latter tribological characteristic, which is widely used in analysis of tests performed with a pin-on-disk tribometer, provides the arithmetic average for the TWC.

ANN modeling framework

Wear equation in the integral form

In pin-on-disk wear tests, we have $w = V/A$, where A is the contact area. Since the contact area if fixed, the contact pressure $p = L/A$ will be constant if the contact load L is kept constant during the test. Also, it is convenient to operate with the sliding distance $s = vt$, where t is the running time.

Now, we assume that the coefficient of wear k, which enters the differential equation (1), may depend on factors such as material composition, contact pressure, sliding velocity and sliding distance. To fix our ideas, we consider k as a function of two variables c and s, where c may represent either a single variable (e.g. concentration of reinforcement) or a vector of physical variables. So, for what follows, we simply rewrite equation (1) as $dw = k(c,s)pvdt$. Now, by taking into account that $V = Aw$, $L = pA$, and $vdt = ds$, the integration of the above equation yields

$$\frac{V}{L} = \int_0^s k(c,\bar{s})\mathrm{d}\bar{s} \tag{2}$$

where $\bar{s}$ is the integration variable.

Evidently, the differentiation of equation (2) with respect to s yields

$$k(c,s) = \frac{1}{L}\frac{\mathrm{d}V}{\mathrm{d}s} \tag{3}$$

Thus, the true wear coefficient can be simply defined as the ratio between the derivative of the wear volume with respect to the sliding distance and the contact load.

ANN modeling of accumulated wear

Now, the wear equation (2) is employed to construct an ANN model for the relative accumulated wear volume in the form of a single-hidden-layer feed-forward neural network

$$\frac{V}{L} = \sum_{j=1}^{N_\mathrm{h}} w_j^{(2)} h_j + b^{(2)} \tag{4}$$

where h_j is the output of the jth hidden neuron, $w_j^{(2)}$ is its weight, N_h is the number of hidden neurons, and $b_j^{(2)}$ denotes the bias of the output neuron. Making use of the weighted summation of inputs, we obtain

$$h_j = f\left(w_{j0}^{(1)} s + \sum_i w_{ji}^{(1)} c_i + b_j^{(1)}\right) \tag{5}$$

where $f(x)$ is the activation function, which is taken to be the same for all hidden neurons, and $b_j^{(1)}$ denotes the bias of the jth neuron. In our analysis, we employ the sigmoid function $f(x) = [1 + \exp(-x)]^{-1}$.

In this approach (in light of equation (3)), an ANN approximation for the wear coefficient can be obtained by differentiating equation (4) as

$$k(c,s) = \sum_{j=1}^{N_\mathrm{h}} w_{j0}^{(1)} w_j^{(2)} \left(h_j - h_j^2\right) \tag{6}$$

where h_j is given by (5), and we used the derivative of the sigmoid activation function $f'(x) = f(x)(1 - f(x))$.

Specific wear rate

Usually, experimental data regarding sliding wear are characterized in terms of the SWR, which is defined as the ratio of volume loss V to the product of load L and sliding distance s. In other words, we have $\mathrm{SWR} = w/(ps)$, where $w = V/A$ and $p = L/A$. Hence, equation (2) implies

$$\mathrm{SWR} = \frac{1}{s}\int_0^s k(c,\bar{s})\mathrm{d}\bar{s} \tag{7}$$

so that the SWR coincides with the integral arithmetic average of the true wear coefficient.

On the other hand, from equation (4), it follows that

$$\mathrm{SWR} = \frac{1}{s}\left(\sum_{j=1}^{N_\mathrm{h}} w_j^{(2)} h_j + b^{(2)}\right) \tag{8}$$

If the SWR is sensitive to the value of sliding distance, then it will provide an average measure for the variable coefficient of wear. Observe also that equation (1) determines the intensity of wear $\dot{w}$, which is assumed to be proportional to k, so that equation (2) connects k with w, which is a sort of extensive variable.

Validation of the ANN modeling approach

Dry wear of friction material against cermet coatings

First, we consider the pin-on-disk studies of running-in performed by Federici et al.[26] on commercial brake friction material under dry sliding conditions at a sliding velocity of 1.57 m/s with the nominal contact pressure of 1 MPa. Figure 3(a) shows their experimental data for the variation of wear volume loss and a fit using a simple ANN model [1-3-1] with the following weights and biases

$$w^{(1)} = \begin{matrix} 0.001 \\ 1.823 \\ 12.181 \end{matrix}, \quad b^{(1)} = \begin{matrix} 0.331 \\ -0.049 \\ 2.66 \end{matrix}, \quad w^{(2)} = \begin{matrix} -12.402 \\ 2.313 \\ 6.941 \end{matrix},$$
$$b^{(2)} = -0.394$$

The corresponding ANN prediction is presented in Figure 3(b) for the wear volume rate defined as

$$W = \frac{\mathrm{d}V}{\mathrm{d}s}. \tag{9}$$

We note that in light of equation (3), we have $W = Lk$, where k is the true wear coefficient.

Based on the experimental data for the wear volume V_n taken at the time moments t_n, the wear volume rate can be approximately evaluated as

$$W(t_n) \approx \frac{V_n - V_{n-1}}{v(t_n - t_{n-1})} \tag{10}$$

where v is the sliding distance. It should be emphasized that equation (10) is approximate, and this can be seen from Figure 3(b), where the finite-difference derivative has been evaluated for the ANN model (see triangle symbols).

Further, recall that $\mathrm{SWR} = V/(Ls)$, so that $V/s = L \cdot \mathrm{SWR}$. At the same time, equation (10) can

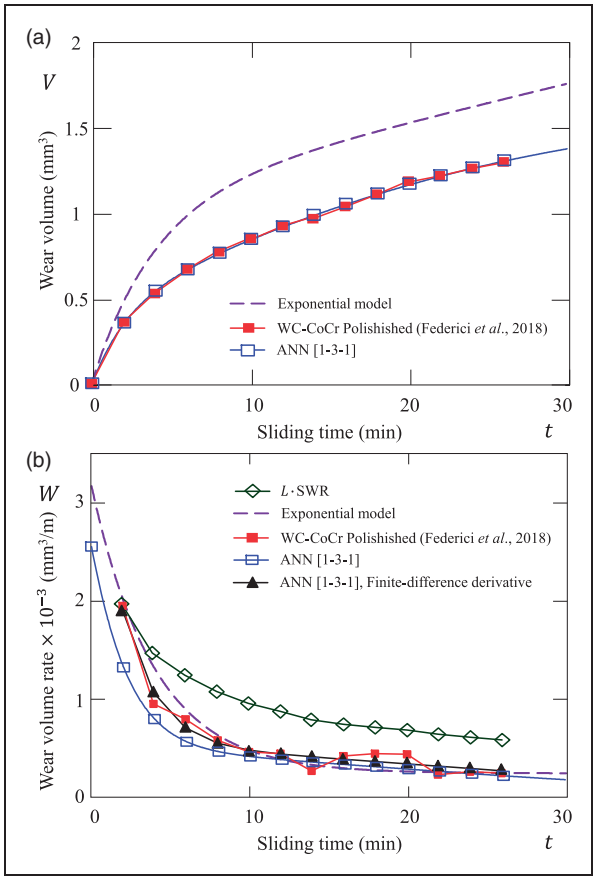

Figure 3. Wear loss volume (a) and wear rate (b) of pins as a function of the sliding time for mechanically polished discs. ANN: artificial neural network; SWR: specific wear rate.

be rewritten as $W \approx \Delta V/\Delta s$. Figure 3(b) shows that in the running-in stage, the SWR (see rhombus symbols) does not estimate well the variable wear rate (shown by empty square symbols).

Moreover, making use of the exponential model,[27] Federici et al.[26] approximated the wear volume rate as

$$W = A_1 \exp(-t/\tau_1) + W_\infty \tag{11}$$

with the coefficients $\tau_1 = 3.96$ (min), $A_1 = 2.93 \times 10^{-3}$ and $W_\infty = 2.39 \times 10^{-4}$ (mm^3/m).

The integration of equation (11), in view of (9), gives the approximation

$$V = v\{W_\infty t + A_1\tau_1[1 - \exp(-t/\tau_1)]\} \tag{12}$$

The prediction of the exponential model (12) for the wear volume is shown in Figure 3(a). The drastic difference with the experimental data for V can be explained by the overestimated value for A_1, which, in turn, is a consequence of the approximate nature of equation (10), especially in the initial interval of rapid volume increase.

One of the benefits of the exponential model (11) is that it provides the approximate value W_∞ for the steady-state wear rate. At the same time, the ANN approximation (3) for the wear coefficient should not be used outside the interval of fit. Therefore, provided that the steady-state regime of wear has been reached in some time interval t_1, t_2, the following approximation for the steady-state wear rate can be recommended

$$W_\infty \simeq \frac{V(t_2) - V(t_1)}{v(t_2 - t_1)} \tag{13}$$

Correspondingly, in light of equation (3), we obtain the steady-state wear coefficient

$$k_\infty \simeq \frac{V(s_2) - V(s_1)}{L(s_2 - s_1)} \tag{14}$$

where $V(s)$ is given by the ANN model (4).

In the case under consideration, taking $t_1 = 23$ min and $t_1 = 25$ min, the ANN models give $W(t_1) = 2.47 \times 10^{-4}$ and $W(t_2) = 2.25 \times 10^{-4}$ (mm^3/m), so that equation (13) yields the value $W_\infty = 2.36 \times 10^{-4}$ (mm^3/m), which differs from the exponential model prediction by 1.3%. We also note that equation (14) gives $k_\infty = 8.35 \times 10^{-6}$ (mm^{3}N^{-1}m^{-1}).

Finally, it should be emphasized that, in contrast to regression models like the exponential model (11), one of the benefits of the ANN modeling approach is that it can be readily generalized to account for the variable operational conditions, provided a sufficient amount of experimental data has been collected.

Wear of zirconia reinforced Al–SiC hybrid composites

In their 24 pin-on-disk tests, Arif et al.[28] considered aluminum hybrid composites reinforced with micro-SiC (5 wt%) and nano-zirconia (0, 3, 6, and 9 wt%) under two levels of applied load L (20 and 40 N) and for three values of sliding distance s (300, 600, and 900 m). Using the ANN modeling and linear regression method, the following relation for the wear mass loss m (mg) was established[28]

$$m = -3.50417 + 0.047z\% + 0.010s + 0.058L - 0.00043sz\% \tag{15}$$

Here, z% is the zirconia mass percentage (wt%).

Our ANN model has three inputs (applied load, L, zirconia mass percentage, z%, and sliding distance, s) and four hidden neurons, which amounts to 21 degrees of freedom, and the following weights and biases

$$w^{(1)} = \begin{matrix} 0.001 & 0.259 & 0.046 \\ 1.841 & 0.537 & 0.171 \\ 0.582 & -1.1265 & 0.795 \\ 0.014 & 3.397 & 2.532 \end{matrix},$$

$$b^{(1)} = \begin{matrix} 0.009 \\ 0.383 \\ 2.492 \\ 0.42 \end{matrix}, \quad w^{(2)} = \begin{matrix} -0.827 \\ 0.161 \\ -2.587 \\ 1.779 \end{matrix}, \quad b^{(2)} = 1.078$$

The mean absolute percentage error of the constructed ANN model is 4.72% against 6.65% for the regression model (15).

Equation (15), in light of equation (3), can be used for estimating the wear coefficient by noting that

$$k = \frac{1}{L\rho}\frac{dm}{ds} \tag{16}$$

where ρ is the density of the tested composite material.

In the case under consideration, we readily have

$$\rho(z\%) = \left\{\left(1 - 0.05 - \frac{z\%}{100}\right)\frac{1}{\rho_{\mathrm{Al}}} + \frac{0.05}{\rho_{\mathrm{SiC}}} + \frac{z\%}{100}\frac{1}{\rho_{\mathrm{ZrO_2}}}\right\}^{-1} \tag{17}$$

where $\rho_{\mathrm{Al}} = 2.7$ gcm^{-3}, $\rho_{\mathrm{SiC}} = 3.21$ gcm^{-3}, and $\rho_{\mathrm{ZrO_2}} = 5.89$ gcm^{-3}.

Thus, differentiating equation (15), we obtain

$$k = \frac{1}{L\rho(z\%)}(0.010 - 0.00043z\%) \tag{18}$$

where $\rho(z\%)$ is given by equation (17).

Figure 4 shows the ANN fit to the experimental data. It is clear that while the wear mass loss as a function of the three input parameters is useful for drawing qualitative conclusions, any quantitative estimate for service conditions will require getting rid of the dependence on the sliding distance. The ANN predictions for the wear coefficient are shown in Figure 5 by the solid lines together with the estimates (dashed lines) extracted from the regression model (15).

Figure 6 shows our predictions for the true wear coefficient (evaluated at $s = 600$ m) as a function of the zirconia mass percentage obtained from the experimental data.[28] It is interesting to observe that the wear coefficient decreases with increasing contact load. This fact implies that the Archard–Kragelsky model, which assumes the power-law dependence of

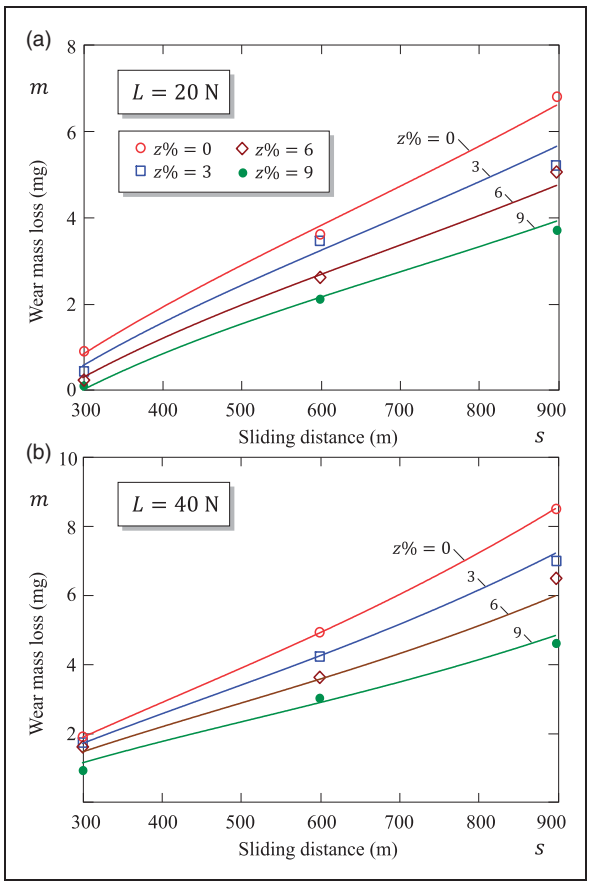

Figure 4. Comparison of measured data[28] and ANN-predicted trends for the wear mass loss versus the sliding distance for the two values of the applied load $L = 20$ N (a) and $L = 40$ N (b) for different values of the percentage concentration of reinforcement.

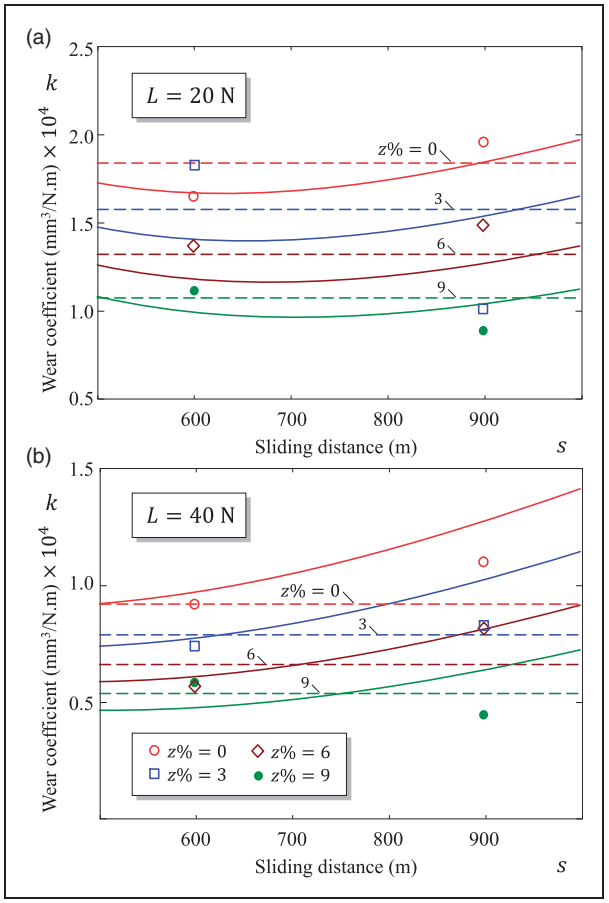

Figure 5. Predictions of the linear regression model (dashed lines), the ANN model (solid lines), and the SWR-based approximations (dot symbols) for the wear coefficient as a function of the sliding distance for the two values of the applied load $L = 20$ N (a) and $L = 40$ N (b) for different values of the mass percentage of zirconia reinforcement.

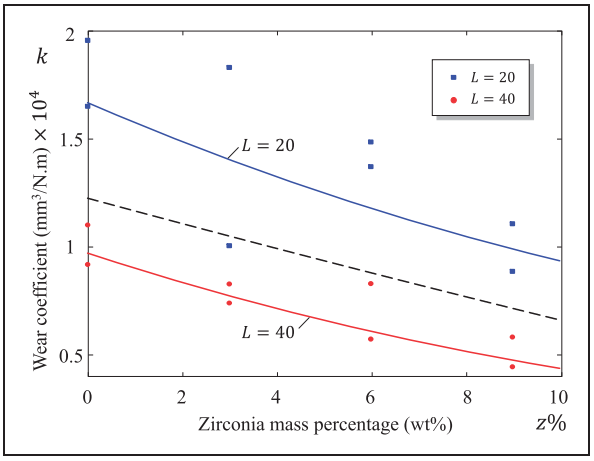

Figure 6. Predictions of the linear regression model (dashed line), the ANN model (solid lines), and the SWR-based approximations (dot symbols) for the wear coefficient as a function of the zirconia mass percentage.

the wear rate $\dot{w}$ on the contact pressure p seems to be more appropriate than Archard's equation (1).

Abrasive wear of aluminum alloy matrix composites

To illustrate the developed theoretical framework, we consider experiments conducted by Canakci et al.[25,29] on the abrasive wear of AA2014 aluminum alloy matrix composites reinforced with B_4C particles. Their sliding wear tests were performed against an abrasive suspension mixture under constant load, $L = 92\,\mathrm{N}$, and linear sliding velocity, $v = 0.314\mathrm{m/s}$. The experimental data from 30 tests were grouped into 20 training and 10 test data, so that $N_{\mathrm{train}} = 20$ and $N_{\mathrm{test}} = 10$. For the samples of varying volume fraction of particles ($c = 0, 2, 3, 6, 9$, and $V(\mathrm{mm}^3)$) the wear volume loss, V (mm^3), was measured and, then, the specific wear rate was calculated using the equation $\mathrm{SWR} = V/(Lvt)$. Also, note that the surface roughness of the contact surface was evaluated in Canakci et al.[25] after each of the wear tests using the surface texture parameter Ra (μm).

A two-hidden-layer MLP with two inputs (sliding time and volume fraction), three outputs (volume loss, specific wear rate, and surface roughness) was constructed by Canakci et al.[25] to study the effect of the sliding time and volume fraction of reinforcement. With four neurons in the first hidden layer and three neurons in the second hidden layer, their ANN architecture [2-4-3-3] amounts to 13 degrees-of-freedom per output.

The predictions of our neural network model [2-3-1] with 13 fitting parameters

$$w^{(1)} = \begin{matrix} -104.3 & 2.964 \\ -2.253 & 1.896 \\ 4.647 & 1.25 \end{matrix}, \quad b^{(1)} = \begin{matrix} 15.6 \\ -0.312 \\ 1.536 \end{matrix},$$

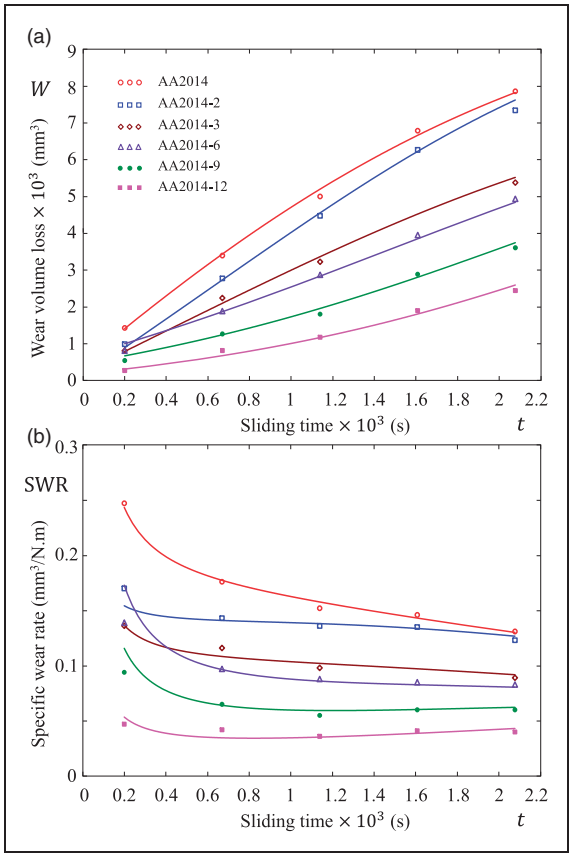

Figure 7. (a) Comparison of measured data[25] and ANN-predicted trends for the wear volume loss versus the sliding time; (b) comparison of measured data and ANN-predicted trends for the specific wear rate loss versus sliding time (for the same legend as in Figure 7(a)).
SWR: specific wear rate.

$$w^{(2)} = \begin{matrix} 2.703 \\ 8.828 \\ 31.48 \end{matrix}, \quad b^{(2)} = -31.86$$

($\mathrm{MAPE}_{\mathrm{train}} = 5.217\%$ and $\mathrm{MAPE}_{\mathrm{test}} = 5.387\%$) for wear volume loss and SWR are presented in Figure 7. It is to emphasize that the SWR curves are drawn by using equation (8) based on the ANN model for wear volume loss, whereas in Canakci et al.[25] the latter is included into the number of ANN outputs.

The main advantage of the developed approach lies in the possibilities to intrinsically analyze the variation of wear coefficient (see Figure 8). It is important to highlight that the SWR represents an approximation for the true wear coefficient, as it can be seen from the comparison of Figures 8 and 7(b). This, in particular, means that the SWR can be used for estimating the coefficient of wear, but only with care taken to provide stabilization of the wear intensity.

Dry sliding wear of Inconel 600 alloy

As yet another example, we consider the experimental results of Banker et al.[30] on 27 pin-on-disk tests whose

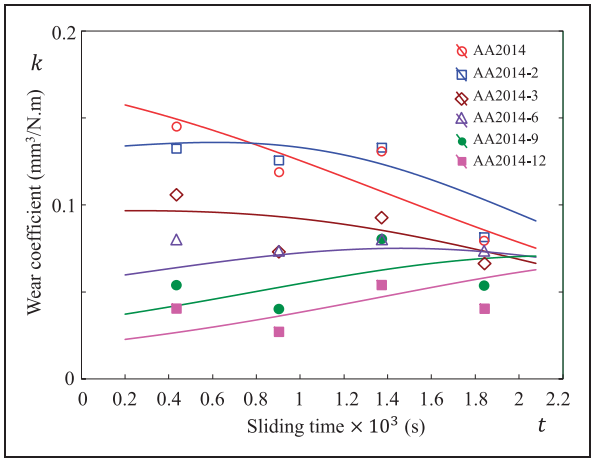

Figure 8. ANN-based predicted variation of the wear coefficient with sliding time for B_4C particle-reinforced composites.

parameters were determined by the Taguchi method for the following four inputs: load, L (N), rotational speed, ϖ (r/min), wear track diameter, D (mm), and pin heating temperature, T (°C). It should be emphasized that all wear tests were conducted for the same duration (7 min). The following linear regression model was obtained for the linear wear (in μm)[30]

$$w = -22.7 + 1.53L + 0.0390\varpi + 0.806D - 0.0716T \tag{19}$$

We recall that the sliding velocity can be evaluated as $v = \omega D/2$, where, in turn, the angular velocity (in rad/s) is given by $\omega = (2\pi/60)\varpi$.

Our ANN model has three inputs (L, T, and sliding distance, s) and four hidden neurons, which amounts to 21 fitting parameters

$$w^{(1)} = \begin{matrix} 0.006 & -1.752 & -3.345 \\ 2.997 & 8.769 & 3.586 \\ 32.57 & -0.038 & -2.318 \\ 4.113 & -13.33 & 2.382 \end{matrix}, \quad b^{(1)} = \begin{matrix} 0.072 \\ -5.772 \\ -33.08 \\ -2.174 \end{matrix},$$

$$w^{(2)} = \begin{matrix} 93.84 \\ 22.4 \\ 26.06 \\ 18.77 \end{matrix}, \quad b^{(2)} = -18.83$$

The weighted absolute percentage error (WAPE) of the constructed ANN model is 1.45% against 3.84% for the regression model (19). Figure 9 shows the fitting results for the ANN model for two values of the applied load.

Observe that equation (3) allows to extract the wear coefficient from the ANN model, but as a function of the sliding distance s. In the case under consideration, the latter variable is simply linked to the sliding velocity v, because the duration of each test is taken to be the same, while sliding velocity is adjusted either by the change in the rotational speed ϖ or in the track diameter D. By taking advantage of this circumstance, we obtain the ANN-based hypothesis for the wear coefficient as a function of sliding velocity (see Figure 10). Interestingly, the obtained results illustrate the conclusion drawn in Banker et al.[30] that ϖ and D are the most significant parameters affecting the wear of Inconel 600.

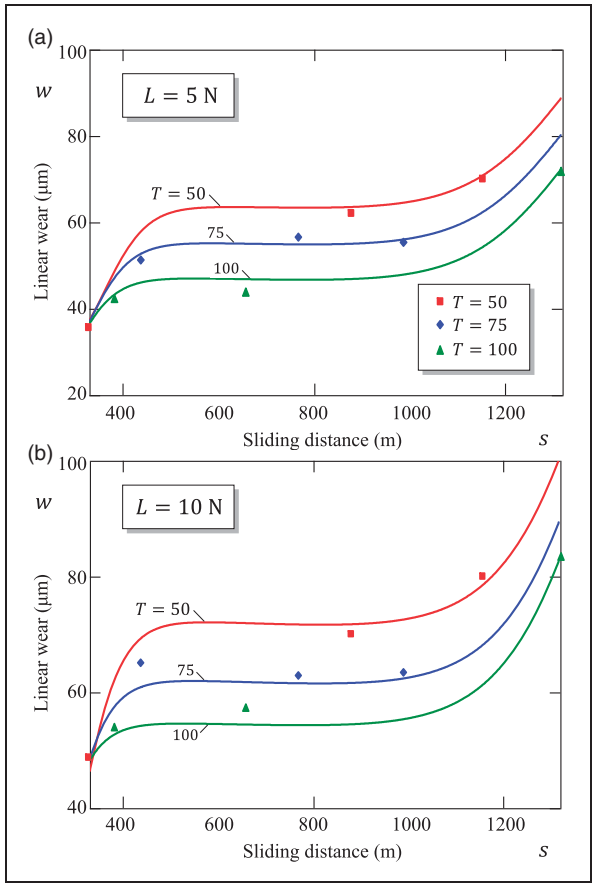

Figure 9. Comparison of measured data[30] and ANN-predicted trends for the linear wear (in microns) versus the sliding distance for the three values of the applied load $L = 5$ N (a) and $L = 10$ N (b) for different values of the pin heating temperature.

Discussion

First of all, it is important to underline that the application of the differential ANN models (4) and (6) can be implemented via standard ANN tools (specifically, the MLP framework and backpropagation learning algorithm[31]). It should be emphasized that, while the present study emphasizes the modeling aspect of the ANN technique, it is shown that the presented ANN models achieve results not worse than their standard counterparts.

Observe that the developed approach can be utilized for analyzing the wearing-in period in the case of constant contact area subjected to sliding.[32] In the case of variable contact area (e.g. in ball-on-disk tribological testing[33]), further study is needed to account for the variability of the contact pressure under a constant normal load. It should be also

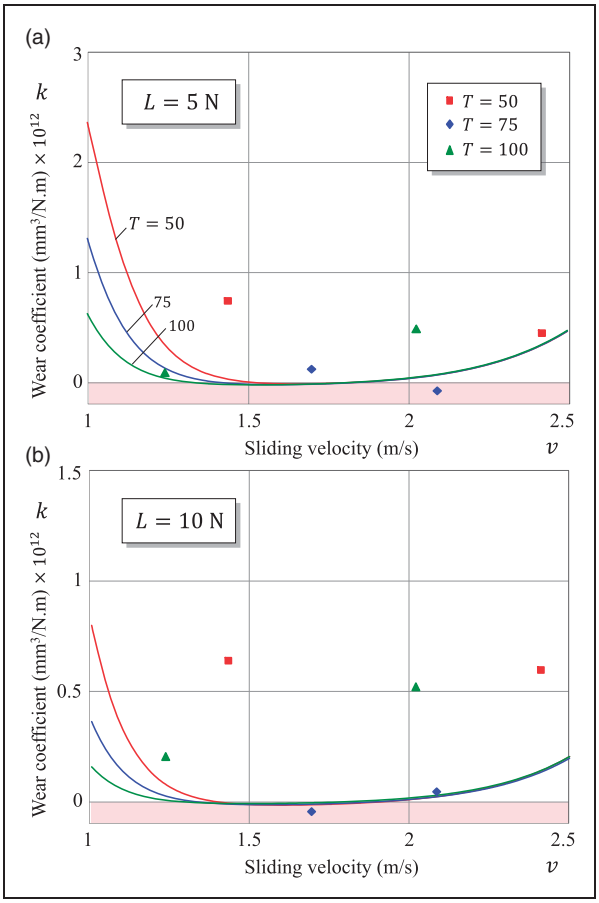

Figure 10. ANN-based predicted variation of the wear coefficient with sliding velocity for Inconel 600 alloy.

emphasized that, generally speaking, an ANN should not be used for predictions outside the range of its training data. Therefore, an extrapolation of the wear coefficient for larger sliding distances is warranted once its variation has been stabilized.

Another critical issue which should be acknowledged is that the wear coefficient may not take negative values, because in sliding wear the wear rate is assumed to be positive. The negative points for the SWR-based wear coefficient observed in Figure 10 are explained by the fact that equation (14) was applied for two sliding distances s_1 and s_2 obtained from tests with different track diameters.

The example considered in the previous section (see, in particular, Figure 10) reveals an interesting aspect of the application of the Taguchi method in conjunction with the ANN analysis. It is recommended to treat the input of sliding time/distance differently compared to the other inputs and not include it into a Taguchi orthogonal array. At the same time, in order to increase the accuracy of determining the wear coefficient via the derivative of the ANN model for the wear loss volume, it is recommended to increase the number of data lines for this input.

Of course, the developed ANN-based modeling framework can be regarded first as a curve-fitting algorithm for convenient analysis of wear data, which depends on the sliding distance. What is more, ANN models can be effectively used for the development of wear transition maps.[34] An insight into the functional wear mechanisms that take place in a tested tribosystem can be gained provided the wear data includes relevant information, such as characteristics of surface roughness[25] or debris features.[35]

It is to note that in the presented analysis it was tentatively assumed that only the wear of pin is accounted for in the total wear volume loss. When substantial wear is experienced by the disc as well (which, for instance, can be determined by means of surface topography analysis[36]), then the sliding distance per unit contact area takes on a different meaning for each body. If n denotes the number of rotations of a cylindrical pin of radius a, sliding along a circular track of diameter D, then the pin sliding distance, evidently, is given by $n\pi D$, which corresponds to the contact area πa^2. At the same time, the disc area which is exposed to wear has the area equal to $2\pi aD$ (for the simplicity's sake we assume that the approximation of small pin applies, that is $a = D/2$). However, the time of wear per one cycle will be different across this annular wear track, and therefore it can be shown (under the assumption of constant contact pressure, which is the case in the steady state) that the equivalent disk distance, which corresponds to the annular track area $2\pi aD$, will be $n\pi a/2$.

So, if in a given pin-on-disk tribosystem, both materials experience wear and the wear of pin affects the wear damage of disc, and vice versa, the developed approach still can be applied, provided the contributions from the both materials to the total wear volume loss can be separated (e.g. if the tribo-pair is composed of different materials, which are easy to distinguish from one another).

Conclusions

The purpose of this research was to establish a robust ANN-based modeling framework for analyzing sliding wear tests performed with a pin-on-disk tribometer. The mathematical modeling approach used to investigate the problem was based on the integral and differential forms of wear equation, which stem from Archard's equation of wear. With regard to the application of ANNs to wear calculations and a comparison with the published data, the primary findings of the work were as follows:

1. When considering the accumulated volumetric wear loss as a function of sliding distance, the wear analysis should distinguish between the TWC and the SWR, the latter of which provides the arithmetic average for the TWC, regarded as a function of the sliding distance.
2. Though the relative sliding velocity can be controlled by either the disc rotational speed or the

track diameter, it is recommended to use the first method, but not a combination of the two.
3. The developed ANN model can be utilized in studies of wearing-in period, which now can be defined as the initial time interval during which the TWC's value is stabilized.

To conclude, in the present communication, the differential ANN-based model is presented for modeling of sliding wear under constant testing conditions, including contact area, contact pressure, and sliding velocity. Examples of sliding wear tests adopted from the literature illustrate the efficiency of the developed constructive approach.

Declaration of Conflicting Interests

The author(s) declared no potential conflicts of interest with respect to the research, authorship, and/or publication of this article.

Funding

The author(s) disclosed receipt of the following financial support for the research, authorship, and/or publication of this article: This work was supported by the National Research Foundation of Korea (NRF) grant funded by the Korean government (MSIT) (No. NRF_2017M2B2A9072449).

ORCID iD

Young S Chai https://orcid.org/0000-0003-1238-3400

References

1. Sha W and Edwards K. The use of artificial neural networks in materials science based research. *Mater Des* 2007; 28: 1747–1752.
2. Wang J, Ma Y, Zhang L, et al. Deep learning for smart manufacturing: methods and applications. *J Manuf Syst* 2018; 48: 144–156.
3. Asteris PG, Moropoulou A, Skentou AD, et al. Stochastic vulnerability assessment of masonry structures: concepts, modeling and restoration aspects. *Appl Sci* 2019; 9: 243.
4. Asteris PG, Apostolopoulou M, Skentou AD, et al. Application of artificial neural networks for the prediction of the compressive strength of cement-based mortars. *Comput Concr* 2019; 24: 329–345.
5. Asteris PG, Armaghani DJ, Hatzigeorgiou GD, et al. Predicting the shear strength of reinforced concrete beams using artificial neural networks. *Comput Concr* 2019; 24: 469–488.
6. Asteris PG and Mokos VG. Concrete compressive strength using artificial neural networks. *Neural Comput Appl*. Epub ahead of print 10 December 2019. DOI: 10.1007/s00521-019-04663-2.
7. Jones SP, Jansen R and Fusaro RL. Preliminary investigation of neural network techniques to predict tribological properties. *Tribol Trans* 1997; 40: 312–320.
8. Velten K, Reinicke R and Friedrich K. Wear volume prediction with artificial neural networks. *Tribol Int* 2000; 33: 731–736.
9. Cavaleri L, Chatzarakis GE, Di Trapani F, et al. Modeling of surface roughness in electro-discharge machining using artificial neural networks. *Adv Mater Res* 2017; 6: 169–184.
10. Psyllaki P, Stamatiou K, Iliadis I, et al. Surface treatment of tool steels against galling failure. In: *MATEC web of conferences*. vol. 188. EDP Sciences, 2018, p. 04024.
11. Cavaleri L, Asteris PG, Psyllaki PP, et al. Prediction of surface treatment effects on the tribological performance of tool steels using artificial neural networks. *Appl Sci* 2019; 9: 2788.
12. Çetinel H, Öztürk H, Çelik E, et al. Artificial neural network-based prediction technique for wear loss quantities in Mo coatings. *Wear* 2006; 261: 1064–1068.
13. Altay O, Gurgenc T, Ulas M, et al. Prediction of wear loss quantities of ferro-alloy coating using different machine learning algorithms. *Friction* 2019; 8: 107–114.
14. Argatov I. Artificial neural networks (ANNs) as a novel modelling technique in tribology: a review. *Front Mech Eng* 2019; 5: 30.
15. Carpenter WC and Barthelemy JF. Common misconceptions about neural networks as approximators. *J Comput Civil Eng* 1994; 8: 345–358.
16. Parikh HH and Gohil PP. Experimental investigation and prediction of wear behavior of cotton fiber polyester composites. *Friction* 2017; 5: 183–193.
17. Haviez L, Toscano R, El Youssef M, et al. Semi-physical neural network model for fretting wear estimation. *J Intell Fuzzy Syst* 2015; 28: 1745–1753.
18. Li D, Lv R, Si G, et al. Hybrid neural network-based prediction model for tribological properties of polyamide6-based friction materials. *Polym Compos* 2017; 38: 1705–1711.
19. Argatov II and Chai YS. An artificial neural network supported regression model for wear rate. *Tribol Int* 2019; 138: 211–214.
20. Archard JF. Contact and rubbing of flat surfaces. *J Appl Phys* 1953; 24: 981–988.
21. Blau PJ and Budinski KG. Development and use of ASTM standards for wear testing. *Wear* 1999; 225: 1159–1170.
22. Blau PJ. *Tribosystem analysis: a practical approach to the diagnosis of wear problems*. Boca Raton, FL: CRC Press, 2016.
23. Páczelt I and Mróz Z. On optimal contact shapes generated by wear. *Int J Numer Methods Eng* 2005; 63: 1250–1287.
24. Gyurova LA and Friedrich K. Artificial neural networks for predicting sliding friction and wear properties of polyphenylene sulfide composites. *Tribol Int* 2011; 44: 603–609.
25. Canakci A, Ozsahin S and Varol T. Prediction of effect of reinforcement size and volume fraction on the abrasive wear behavior of AA2014/B_4C_pMMC$_s$ using artificial neural network. *Arabian J Sci Eng* 2014; 39: 6351–6361.
26. Federici M, Perricone G, Gialanella S, et al. Sliding behaviour of friction material against cermet coatings: pin-on-disc study of the running-in stage. *Tribol Lett* 2018; 66: 53.
27. Schneider EW, Blossfeld DH and Balnaves MA. Effect of speed and power output on piston ring wear in a diesel engine. *SAE Trans* 1988; 97: 1257–1267.
28. Arif S, Alam MT, Ansari AH, et al. Analysis of tribological behaviour of zirconia reinforced Al-SiC hybrid

composites using statistical and artificial neural network technique. *Mater Res Express* 2018; 5: 056506.
29. Canakci A. Microstructure and abrasive wear behaviour of B_4C particle reinforced 2014 Al matrix composites. *J Mater Sci* 2011; 46: 2805–2813.
30. Banker VJ, Mistry JM, Thakor MR, et al. Wear behavior in dry sliding of Inconel 600 alloy using Taguchi method and regression analysis. *Procedia Technol* 2016; 23: 383–390.
31. Rumerlhar D. Learning representation by back-propagating errors. *Nature* 1986; 323: 533–536.
32. Hanief M and Wani M. Modeling and prediction of surface roughness for running-in wear using Gauss-Newton algorithm and ANN. *Appl Surf Sci* 2015; 357: 1573–1577.
33. Kolodziejczyk T, Toscano R, Fouvry S, et al. Artificial intelligence as efficient technique for ball bearing fretting wear damage prediction. *Wear* 2010; 268: 309–315.
34. Srinivasan V, Maheshkumar KV, Karthikeyan R, et al. Application of probablistic neural network for the development of wear mechanism map for glass fiber reinforced plastics. *J Reinf Plast Compos* 2007; 26: 1893–1906.
35. Myshkin NK, Kwon OK, Grigoriev AY, et al. Classification of wear debris using a neural network. *Wear* 1997; 203: 658–662.
36. Dzierwa A, Pawlus P, Zelasko W, et al. The study of the tribological properties of one-process and two-process textures after vapour blasting and lapping using pin-on-disc tests. *Key Eng Mater* 2013; 527: 217–222.